EM–00000

Ballistic Impact of Braided Composites with a Soft Projectile

Gary D. Roberts,[*] J. Michael Pereira,[†] Duane M. Revilock, Jr.,[‡] Wieslaw K. Binienda,[§]

Ming Xie,[**] and Mike Braley[††]

CE Database Subject Headings: composite materials, composite structures, impact tests, aerospace engineering

Abstract

Impact tests using a soft gelatin projectile were performed to identify failure modes that occur at high strain energy density during impact loading. Failure modes were identified for aluminum plates and for composites plates and half-rings made from triaxial carbon fiber braid having a 0/±60° architecture. For aluminum plates, a large hole formed as a result of crack propagation from the initiation site at the center of the plate. For composite plates, fiber tensile failure occurred in the back ply at the center of the plate. Cracks then propagated from this site along the ±60° fiber directions until triangular flaps opened to form a hole. For composite half-rings fabricated with 0° fibers aligned circumferentially, fiber tensile failure also occurred in the back ply. Cracks first propagated from this site perpendicular the 0° fibers. The cracks then turned to follow the ±60° fibers and 0° fibers until rectangular flaps opened to form a hole. Damage in the composites was localized near the impact site, while cracks in the aluminum extended to the boundaries.

Introduction

In a previous paper (Roberts 2002), a test method was proposed for evaluating composite fan case designs as potential lightweight alternatives to the metal structures currently used in commercial jet engines. In the proposed method, a rigid titanium disk is shot from a gas gun and impacts a 91 cm (36 in.) diameter composite ring, as shown in Figure 1. In this test, the disk projectile represents a blade fragment resulting from a blade-out event. The fixed lower mounting of the ring represents the boundary condition at the aft flange of the fan case, and the upper edge of

[*] Materials Engineer, NASA Glenn Research Center, 21000 Brookpark Road, Cleveland, OH 44135
[†] Aerospace Engineer, NASA Glenn Research Center, 21000 Brookpark Road, Cleveland, OH 44135
[‡] Aerospace Engineer, NASA Glenn Research Center, 21000 Brookpark Road, Cleveland, OH 44135
[§] Professor of Civil Engineering, University of Akron, Akron, OH 44325–3905
[**] Lead Design Engineer, General Electric Aircraft Engines, One Neumann Way, Cincinnati OH 45215–6301

the ring represents the forward flange, which is connected to the inlet. Explicit finite element analysis (with no failure) was done to examine impact dynamics at an impact velocity of 183 m/s (600 ft/s). Projectile motion and ring deformation during and after impact are shown in Figure 2. Results of this preliminary analysis identified three time scales of interest. First, the initial contact of the disk with the ring and the subsequent rebound from this point (due mainly to rotation of the rigid projectile) occur at times less than 1 ms. Second, the continued motion of the projectile into the deforming ring and the rebound of the entire projectile from the ring occur over a time of about 1 ms. During this time interval the ring is subjected to the maximum strain energy density in a region near the impact site. Third, propagation of flexural waves around the ring occurs at times greater than 1 ms. Impact of quarter- and half-ring targets with free and fixed boundary conditions were also analyzed in the previous paper (Roberts 2002). Results indicated that the short time (< 1 ms) initial impact dynamics was the same as that in the full-ring test for both free and fixed boundary conditions. The practical implication of this result is that it appears to be feasible to use simpler subsection tests (or flat plate tests) with a rigid projectile to study the local perforation response of the composite ring. This could lead to substantial savings in testing time and cost as long as the impulse provided by a smaller projectile impacting flat plates or ring sections can be shown by analysis to be comparable to the impulse in the full ring test. Although work in understanding this short time local impact problem is continuing, the subject of this paper is deformation and failure during the second time interval described above when the strain energy density is large enough to induce failures such as cracking and delamination even in the absence of perforation. In order to achieve this condition experimentally, a soft gelatin projectile is used instead of a rigid titanium projectile. If a rigid projectile were to be used, perforation of the composite by the projectile would limit the transfer of projectile kinetic energy into strain energy in the composite. It would therefore not be possible to identify failure modes that occur at very high levels of strain energy.

In this paper, experimental results are reported for impact of cylindrical gelatin projectiles on aluminum and composite targets. A first set of tests was performed using flat plates as the targets in order to identify potential failure modes and to provide an estimate of the penetration threshold using a relatively simple test geometry. A second set of tests was then performed using half-rings as targets in order to observe the failure modes and measure the penetration threshold in a curved geometry that is more representative of a fan case. One result of these

[††] Application Engineer, A&P Technology, 4595 East Tech Drive, Cincinnati, OH 45245–1055

experiments was identification of a sequence of failure events in the composites that could not be simulated using the current capabilities of commercial explicit finite element codes. Some promising approaches for performing the analysis are currently being investigated, but the focus of this paper is the experimental results, including a description of the types of failure that will need to be considered in the finite element analysis.

Impact Test Methods

The soft projectiles used in the impact tests were made using a mixture of gelatin and microballoons with a density of 960 kg/m^3. The mixture is cast in the shape of a cylinder 12.7 cm (5 in.) long and 7.0 cm (2.75 in.) in diameter. Figure 3 shows an example of a projectile before and after impact. For impact testing a projectile is mounted in a sabot and shot into a target using a 20.3 cm (8 in.) diameter gas gun. The axis of the cylindrical projectile is aligned along the line of flight, so that the flat end of the cylinder makes first contact with the target. Impact velocity is measured digitally using a high speed video camera with a view perpendicular to the line of flight. During a test the projectile initially flattens into a disk approximately 25.4 cm (10 in.) in diameter before rebounding to the "after impact" shape shown in Figure 3(b). At low velocities the projectile can be recovered in the form shown in Figure 3(b), but at high velocities the projectile is disintegrated into small pieces.

Composites were fabricated by resin infusion of M36 resin (a toughened epoxy system from HEXCEL Composites) into six layers of a triaxial braided T700 carbon fiber preform. The preform was manufactured by A&P Technology, the composites were fabricated by GE Aircraft Engines, and the impact testing was done in the Ballistic Impact Lab at the NASA Glenn Research Center. The braided preform had 12k flat tow fibers in the ±60° (bias) directions and 24k flat tow fibers in the 0° (axial) direction. The fiber volume in each direction was equal, so that both the individual plies and the entire lay-up were quasi-isotropic. A 6 ply lay-up was made with the 0° fibers aligned. The cured composites had a thickness of about 3.2 mm (0.125 in.). Composites were fabricated in the form of 61×61 cm (2×2 ft) flat plates and 112 cm (44 in.) diameter half-rings. A set of 0.180 cm (0.071 in.) thick type 2219 aluminum flat plates were also tested. This thickness was chosen so that the aluminum plates and composite plates would have nearly equal weight per unit area. Figure 4 shows a composite plate still mounted in the fixture after impact. The plate is mounted by bolting through the steel picture frame visible in Figure 4 into a heavy steel backing frame. The plate is held in place by the clamping force of the picture frame. During the test program several modifications were

made to the mounting procedure in order to eliminate slipping of the edges of the plate from the test fixture. Initial tests were done with a 55.9 cm (22 in.) square opening in the frame, which allowed for a 2.54 cm (1 in.) wide clamping area around the plates. With this arrangement, slipping of the edges of the plate was a problem, especially at impact velocities near the penetration threshold. To solve this problem, 0.64 cm (0.25 in.) holes spaced 5.08 cm (2 in.) apart were drilled through the steel fixture and through the plates. Steel pins were then inserted into the holes. These pins can be seen in Figure 4. In addition to the pins, 2.54 cm (1 in.) wide strips of a stainless steel wire mesh were placed between the composite plate and the steel frame. For the most recent series of tests, a thicker frame was made with an opening of 50.8 cm (20 in.) instead of 55.9 cm (22 in.). Grooves were machined into the contacting surfaces of the frame to eliminate the need for the wire mesh. With these modifications to the frame, slipping at the edges of the plates was eliminated for most tests. The effect of slipping on the test results is discussed below. The 112 cm (44 in.) diameter half-ring test fixture is shown in Figure 5. Bolts spaced 2.54 cm (1 in.) apart hold the half-ring in place against thick metal rails on all sides. Slipping of the edges was not a problem with this test fixture.

Impact of Aluminum Plates

An initial set of 4 tests were done on aluminum plates using the 55.9 cm (22 in.) frame opening and impact velocities ranging from 156 m/s (513 ft/s) to 235 m/s (770 ft/s). In this test configuration the clamped area is only one inch wide, and even the use of pins through the plate was insufficient to prevent slipping of the edges out of the frame. Figure 6(a) shows the plate tested at 156 m/s (513 ft/s). Some tearing of the pin holes resulting from slipping is evident in the left edge of the plate in Figure 6(a). The type of damage that occurred was similar for all 4 plates, except that the extent of deformation and the amount of slipping from the frame were much more severe at the higher velocities. Each of the 4 plates had a circular region of extensive plastic deformation at the center that is about the size of the initial contact area and less extensive plastic deformation in the region between the initial contact area and the edges of the plate. The four folds beginning at the corners of the plate and directed at 45° toward the center of the plate are an artifact of the stress field imposed by the square boundary conditions. It was somewhat surprising that the aluminum plates were not penetrated with an impact velocity of 235 m/s (770 ft/s). In order to determine if penetration would occur if the edges of the plate were held tightly in place, two more tests were done on the remaining plates using the new frame with the 50.8 cm (20 in.) opening. This frame allows for a 5.08 cm (2 in.) clamping width at the edges of the plate. A plate tested at 226 m/s (743 ft/s) in this frame is shown in

Figure 6(b). With the edges of the plate now held more tightly in place, penetration did occur along with extensive cracking of the plate. High speed video of the impact event clearly showed crack initiation near the initial contact area and dynamic crack propagation toward the boundaries. Figure 6(b) illustrates the effect of having a high strain energy density in the plate at the onset of failure. A second plate tested at 199 m/s (654 ft/s) was not penetrated by the projectile. However, some slipping occurred at the boundaries, even though the new test frame was used. Further testing would therefore be needed to determine the penetration threshold in a test where the boundaries are held completely fixed.

Impact of Composite Plates

Eight composite plates were tested with impact velocities ranging from 103 m/s (338 ft/s) to 198 m/s (648 ft/s). The failure mode for the composite plates differed from that for the aluminum plates in several ways. First, when tested at velocities below the penetration threshold, the composites did not have a permanent deformation analogous to the plastic deformation in the aluminum plates. Second, the penetration threshold was lower for the composite plates. Third, when tested above the penetration threshold, the damage did not propagate beyond an area approximately the size of the initial contact area. Slipping at the edges of the plates was a problem in the initial tests using the frame with the 55.9 cm (22 in.) opening and only the bolts around the edges to hold the plates in place. Addition of pins through the steel frame and the composite plate reduced the slipping considerably. However, elongation of the holes in the composite and cracks emanating from the holes in some tests indicated that slipping was probably not completely eliminated. Using data only from tests in which the slipping appeared to be very small, the penetration threshold was determined to be between 150 m/s (491 ft/s) and 161 m/s (528 ft/s). Figure 7 shows the front and back surfaces of the composite plate tested at 150 m/s (491 ft/s). In Figure 7(a) the small whitened circular region at the center of the plate is the initial contact area. The larger, less distinctive, whitened area is the region over which the gelatin projectile was spread when it was completely flattened into a disk before rebounding. There is no visible damage on the front side of the plate. However, in Figure 7(b) there appears to be a small circular region of fiber tensile failure at the center of the back side of the plate. A magnified view of this damage is shown in Figure 7(c). This type of damage in the back ply is reasonable since the maximum strain should occur at this point. Fiber fracture also occurred on the back of other composite plates tested at velocities well below the penetration threshold. It was not possible to determine the threshold velocity for the onset of this failure mode because of the limited number of

plates available and because the test results can not be considered to be reliable in tests where slipping occurs at the boundaries. A lower bound for this threshold can be estimated from results of one test at 103 m/s (338 ft/s). There was no visible damage in this plate after the test. However, high speed video showed the projectile to be misaligned and partially torn before impact. Further testing would be needed to establish a threshold for onset of detectable damage.

At impact velocities of 161 m/s (528 ft/s) and above, the projectile perforated the composite plates with the damage pattern shown in Figure 8. The plate in Figure 8 was tested at 192 m/s (629 ft/s). Penetration is initiated at the center of the plate where fiber tensile failure has occurred on the back ply. Cracks then propagate along the ±60° bias fiber directions. When these cracks extend beyond the initial contact area, triangular flaps fold back along 0° axial fibers. Two remarkable results are that the cracks do not propagate far from the initial impact area and that there is no apparent delamination between plies. It was anticipated that these damage modes would be present and would have to be controlled by the use of buffer strips or other methods. The damage tolerance demonstrated in these tests suggests that such methods for limiting crack growth may not be needed in fan case structures. A possible contributing factor to the damage tolerance is that the interlaminar stresses available to induce damage are small because the triaxial braid is quasi-isotropic within each ply. This issue is currently being investigated both experimentally and by analysis.

Impact of Composite Half-Rings

Two half-rings were tested using the fixture shown in Figure 5. The half-ring composites were fabricated so that the 0° fibers are oriented circumferentially in the fixture. The damaged region after a test at 150 m/s (492 ft/s) is shown in Figure 9. Because the damage is localized around the initial contact area, it is possible to perform three separate impact tests on each half-ring. Slipping of the edges out of the fixture was not a problem in any of these tests. The penetration threshold was between 133 m/s (436 ft/s) and 138 m/s (454 ft/s). This is lower than the range of 150 m/s (491 ft/s) to 161 m/s (528 ft/s) determined for the composite flat plates. The penetration thresholds are not expected to be the same for the flat plates and the half-rings because the stress state induced in the composite by impact is different for the different geometries. Some of the failure modes observed in the flat plates also occurred in the half-rings. For velocities below the penetration threshold, a small circular region of fiber fracture occurs in the back ply directly behind the center of the initial impact area. Similar to the flat plates, this region of fiber fracture is the initiation site for crack propagation when the impact velocity exceeds the penetration threshold. However, in the half-ring tests the cracks initially propagate from the initiation site in a direction transverse to the 0° fibers rather than along the ±60° fibers. As the cracks reach a location near the edge of the initial impact site, each of the transverse cracks split into two cracks that travel a short distance along the ±60° directions. These cracks then turn again to travel along 0° fibers. Square flaps then open by folding along a line transverse to the 0° fibers. Similar to the flat plates, the damaged area is only slightly larger than the initial contact area.

Conclusion

The approach of using a soft projectile to identify failure modes induced by high strain energy density during impact loading was successfully demonstrated. The large hole induced by penetration of the aluminum plate illustrates how excessive damage can occur when strain energy drives dynamic crack propagation without limit toward the boundaries. Composites fabricated with the quasi-isotropic triaxial braid fiber architecture were surprisingly damage tolerant in both the flat plate and half-ring configurations. Crack propagation was arrested when flaps folded back leaving a damaged region only slightly larger than the initial impact area. No delamination was evident by visual examination. This high level of damage tolerance is a critical property for fan cases in commercial jet engines.

Although the flat plate tests are potentially less expensive and easier to perform than the half-ring tests, there are several issues that limit the usefulness of the data from these tests. First, the results are strongly influenced by slipping at the boundaries. Second, the flat plates did not exhibit all of the damage modes that occurred in the half-rings. In particular, transverse tearing across fibers did not occur in the flat plates. Third, the fabrication method for flat plates may not adequately represent the method that would ultimately be used to fabricate a ring structure. Because of these issues impacting of curved targets, such as the half-rings, is a preferred method when the goal is to evaluate materials for use in fan case structures. The ability to perform three tests on each half-ring somewhat offsets the increased difficulty of mounting the composite in the fixture. Both the flat plate tests and the half-ring tests have provided useful information for materials evaluation and for guiding the development of analysis methods. However, a full-ring configuration would better represent a fan case structure, and efforts to develop this method are continuing.

Reference

Roberts, G.D., Revilock, D.M., Binienda, W.K., Nie, W.Z., Mackenzie, S.B., and Todd, K.B. (2002). "Impact Testing and Analysis of Composites for Aircraft Engine Fan Cases." *J. Aerospace Engineering*, Vol. 15, No. 3, 104–110.

Figures List

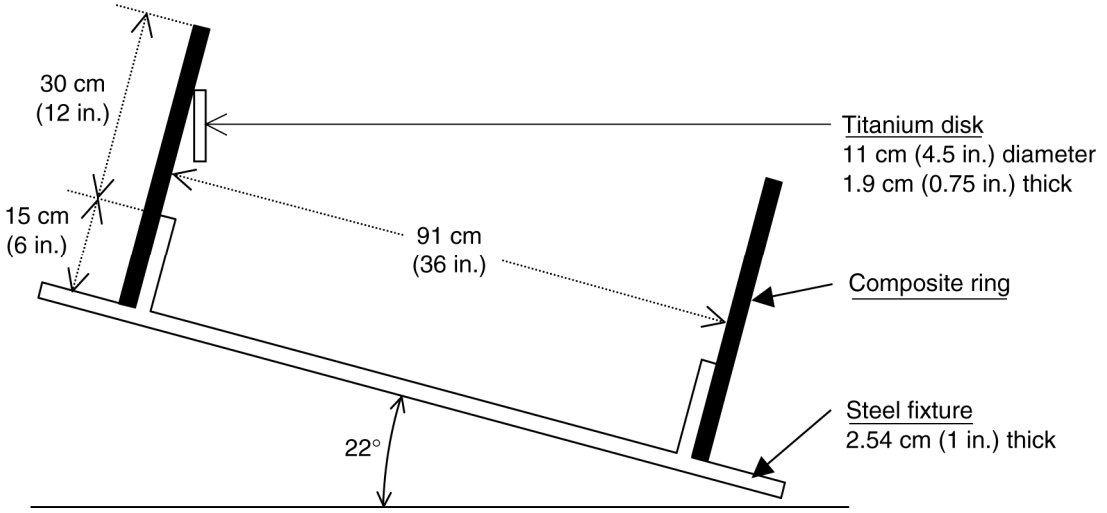

Fig. 1. 91 cm (36 in.) diameter full-ring subcomponent test.

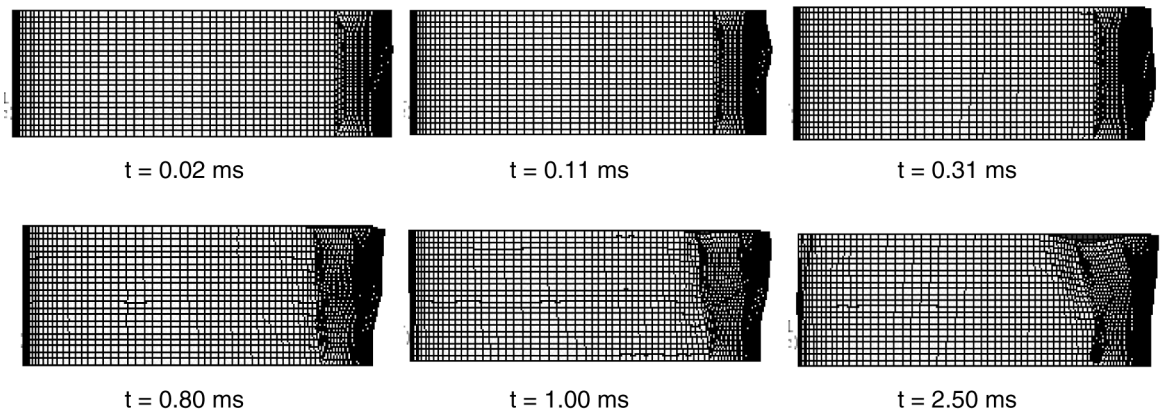

Fig. 2. Deformation of 91 cm (36 in.) composite ring after impact at 183 m/s (600 ft/s).

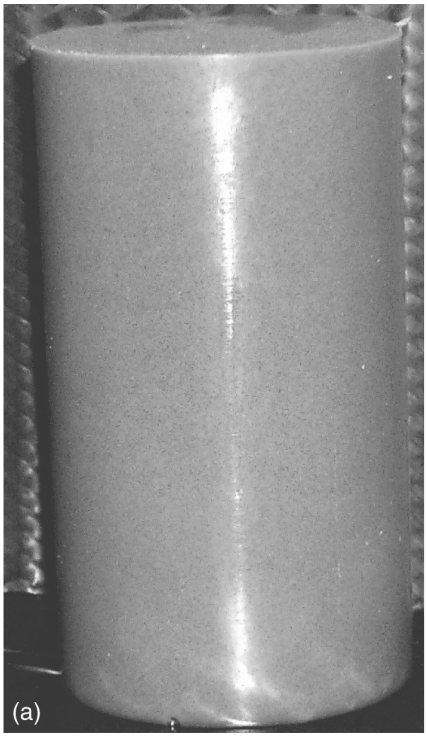

Fig. 3. Gelatin projectile. (a) Before impact. (b) After impact.

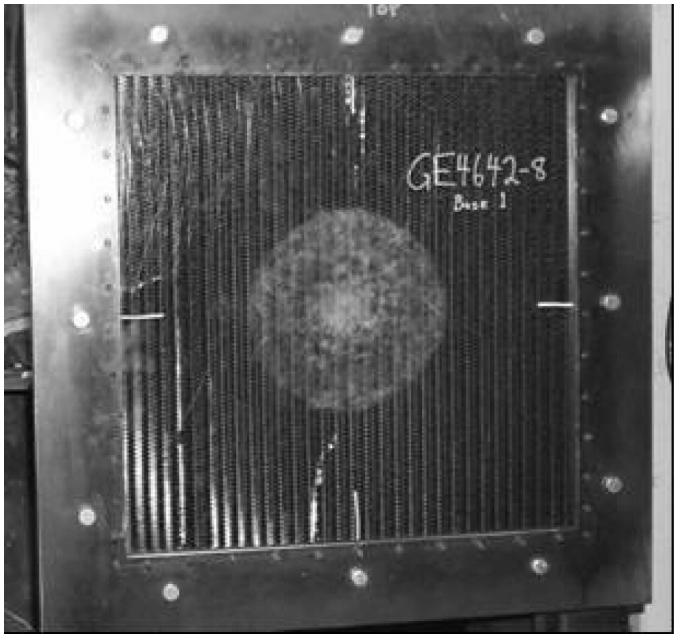

Fig. 4. Test fixture for the 61×61 cm (2×2 ft) flat composite plates.

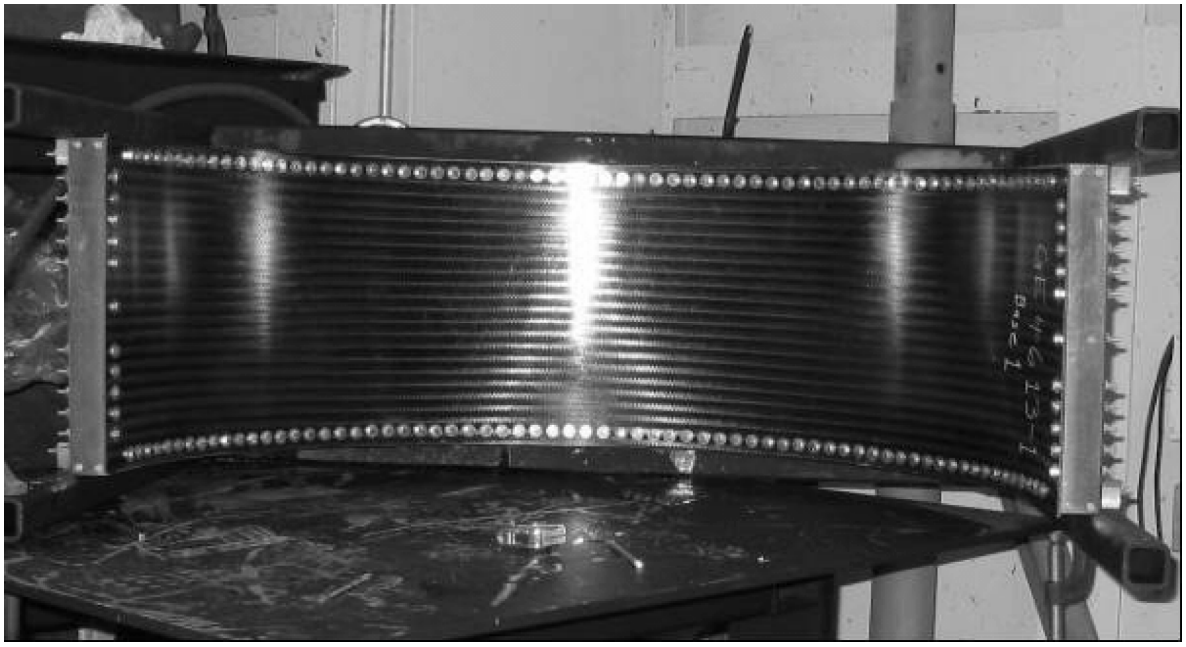

Fig. 5. Test fixtures for the 112 cm (44 in.) diameter composite half-rings.

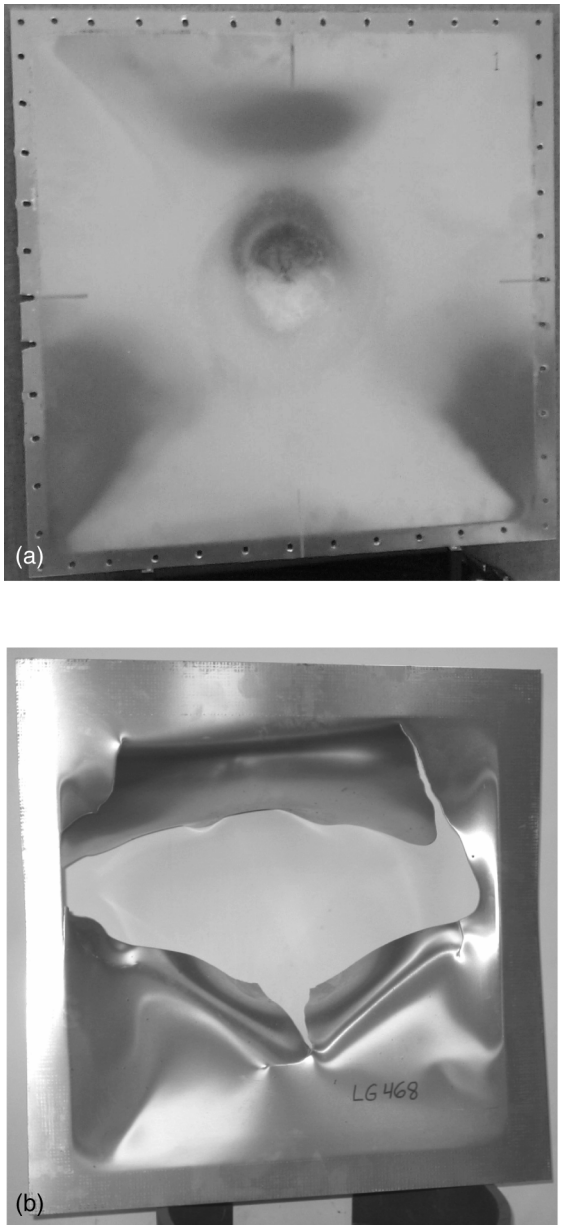

Fig. 6. Aluminum panels after impact. (a) 156 m/s (513 ft/s). (b) 226 m/s (743 ft/s).

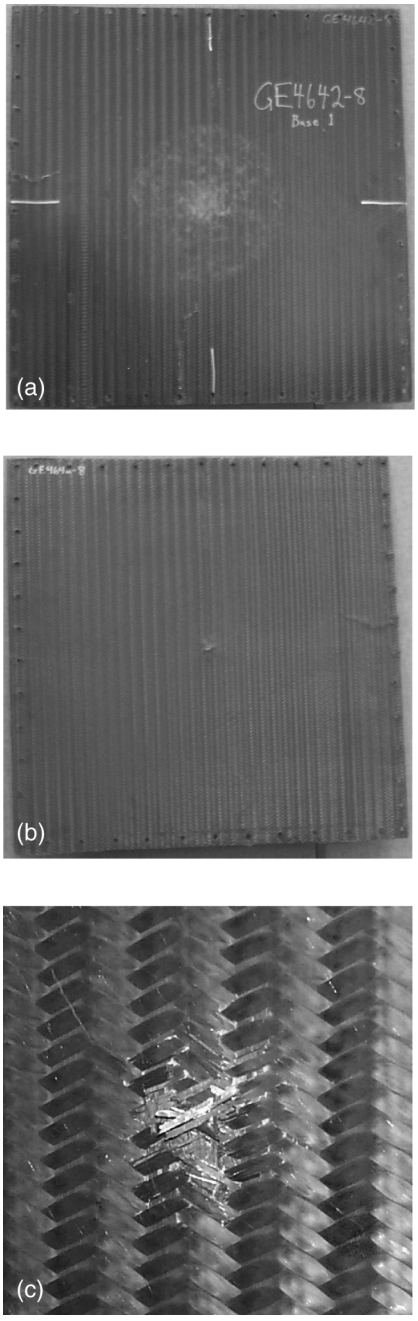

Fig. 7. Composite flat panels after impact at 150 m/s (491 ft/s). (a) Front. (b) Back. (c) Back, close-up.

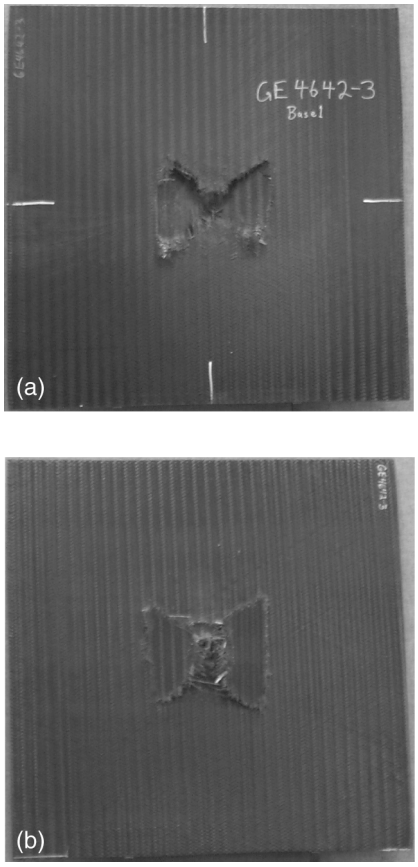

Fig. 8. Composite flat panels after impact at 192 m/s (629 ft/s). (a) Front. (b) Back.

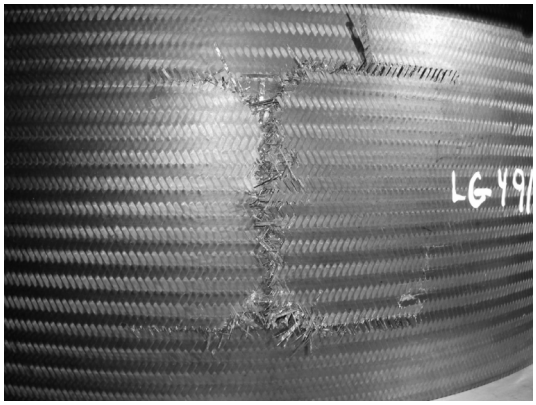

Fig. 9. Composite half-ring after impact at 150 m/s (492 ft/s).